Ground Water Monitoring&Remediation

# Modeling Volatile Chemical Transport, Biodecay, and Emission to Indoor Air

*by Jack C. Parker*

## Abstract

A model is presented for estimating vapor concentrations in buildings because of volatilization from soil contaminated by nonaqueous phase liquids (NAPL) or from dissolved contaminants in ground water. The model considers source depletion, diffusive-dispersive transport of the contaminant of concern (COC) and of oxygen and oxygen-limited COC biodecay. Diffusive-advective transport through foundations and vapor losses caused by foundation cross-flow are considered. Competitive oxygen use by various species is assumed to be proportional to the product of the average dissolved-phase species concentration and a biopreference factor. Laboratory and field data indicate the biopreference factor to be proportional to the organic carbon partition coefficient for the fuel hydrocarbons studied. Predicted indoor air concentrations were sensitive to soil type and subbase permeability. Lower concentrations were predicted for buildings with shallow foundations caused by flushing of contaminants by cross-flow. NAPL source depletion had a large impact on average exposure concentration. Barometric pumping had a minor effect on indoor air emissions for the conditions studied. Risk-based soil cleanup levels were much lower when biodecay was considered because of the existence of a threshold source concentration below which no emissions occur. Computed cleanup levels at NAPL-contaminated sites were strongly dependent on total petroleum hydrocarbon (TPH) content and COC soil concentration. The model was applied to two field sites with gasoline-contaminated ground water. Confidence limits of predicted indoor air concentrations spanned approximately two orders of magnitude considering uncertainty in model parameters. Measured contaminant concentrations in indoor air were within model-predicted confidence limits.

## Introduction

An increased emphasis on risk-based corrective action at contaminated sites has made the availability of accurate methods for estimating potential exposure critically important. A particularly problematic exposure pathway involves inhalation of contaminants that volatilize from soil or ground water into buildings. A variety of models have been proposed to estimate volatile emissions from soils. The model of Jury et al. (1990) and the SESOIL and VLEACH models have been used to compute vapor fluxes to outdoor air. These models consider finite dissolved contamination sources, but are not directly applicable to nonaqueous phase liquid (NAPL) sources. VLEACH does not consider biodecay, whereas SESOIL and the Jury model approximate biodecay using a first-order rate equation.

Johnson and Ettinger (1991), Little et al. (1992), and Sanders and Stern (1994) presented models for volatilization to indoor air. Little et al. (1992) assumed an infinite source duration, which will lead to overestimation of average exposure. Johnson and Ettinger (1991) discussed models for both an infinite source and a finite NAPL source. The infinite source formulation has been widely adopted for routine risk-assessment studies. Sanders and Stern (1994) considered a finite dissolved-phase source, but did not model a NAPL source. Johnson and Ettinger (1991) and Little et al. (1992) did not consider biodecay, and Sanders and Stern (1994) incorporated a first-order biodecay term. Indoor air intrusion models have been presented recently by Johnson et al. (1998, 1999) and Hers (2000) that also consider first-order biodecay. First-order biodecay models are attractively simple, but the apparent rate coefficients are highly variable due to the influences of many site-specific factors. For example, Johnson et al. (1999) reported that an apparent first-order coefficient of 22 $d^{-1}$ matched vapor transport data from a specific site, while noting that coefficients of 0.01 to 0.001 $d^{-1}$ are commonly observed in ground water.

Limitations of empirical first-order decay models have been an impetus for development of more physically based electron receptor-limited ground water biodecay models (Borden and Bedient 1986; Rifai et al. 1988). An analysis of oxygen-limited biodecay in the unsaturated zone has been presented by Lahvis et al. (1999), which indicates biodecay rates are markedly affected by the distribution of available oxygen among multiple degrading species. Neglecting biodecay and/or source depletion over time will lead to overestimation of human health risk from vapor exposure.

The Johnson and Ettinger (1991) model considers impedance to building intrusion associated with advection through the soil and to advection and diffusion through the building foundation. Other vapor intrusion models mentioned disregard these factors and consider simple dilution with building air

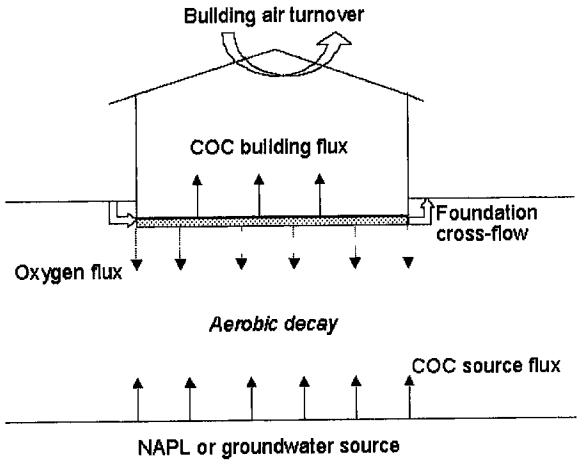


Figure 1. Overview of model components.

turnover. No reported models consider possible reductions in building intrusion from horizontal airflow beneath the building induced by wind. Further, none of the models cited consider vapor transport induced by barometric pressure fluctuations. This phenomenon, commonly referred to as "barometric pumping," has been recognized for many years, although quantitative approaches have been developed only relatively recently (CDM 1986; Nilsen et al. 1991; Auer et al. 1996). In certain circumstances, fluxes due to barometric pumping may exceed those from molecular diffusion (e.g., fine-grained soils with a deep water table). Effects of barometric pressure fluctuations on radon gas entry into buildings have been studied extensively (Clements and Wilkening 1974; Schery et al. 1984; Tsang and Narasimhan 1992; Robinson and Sextro 1997).

This paper presents a model to assess human exposure and health risk associated with volatile chemical emissions to indoor air from contaminated soil or ground water, considering a finite source mass, vapor transport due to advection, diffusion, and barometric pumping; oxygen-limited biodecay; and building underflow (Figure 1). A theory is presented and tested with data in the literature to assess competitive oxygen use in multispecies systems. Example applications are presented involving volatilization from NAPL and ground water sources. Results from two field studies are employed to evaluate the field performance of the model.

## Model Description

### Source Zone Model

The source zone is the region in the subsurface that serves as the source of volatile chemicals. Two types of sources are considered: (1) dissolved chemicals present at the water table under a building or (2) residual NAPL present in the soil under a building.

#### *Dissolved Ground Water Source*

For the case of dissolved chemicals at the water table, equilibrium partitioning is assumed between ground water and immediately overlying soil vapor. If changes in dissolved phase concentration in ground water over time are considered, an exponential function is assumed. The source vapor concentration of the contaminant of concern (COC) at time (t) is calculated as

$$C^{v}_{source} = H_{coc} C^{w}_{source} \exp( - \alpha_{coc} t) \quad (1)$$

where $C^{v}_{source}$ is the equilibrium vapor concentration at the source at any time, $C^{w}_{source}$ is the current average aqueous-phase concentration of COC at the water table, $\alpha_{coc}$ is the net rate of change in the ground water COC concentration as a result of all processes in the ground water (e.g., source depletion, dispersion, and biodecay), and $H_{coc}$ is a dimensionless Henry's constant. Unlu et al. (1992) derived an expression for $\alpha_{coc}$ for a single soluble species in a NAPL mixture in contact with ground water, which is a function of ground water velocity, total NAPL volume, COC mass fraction, COC solubility, and a mass-transfer coefficient. If an adequate time series of dissolved concentration data are available, the rate coefficient $\alpha_{coc}$ may be estimated from field dissolved concentration data by regression. Employing $\alpha_{coc} = 0$ represents a constant ground water concentration over time, which may be employed if data are not available to define source depletion. Averaging over an exposure period from t = 0 to $t_{exp}$ yields an average vapor-phase source concentration, $C^{coc}_{source}$, given by

$$C^{coc}_{source} = \frac{H_{coc} C^{w}_{source}}{\alpha_{coc} t_{exp}} \left(1 - \exp( - \alpha_{coc} t_{exp})\right) \quad (2)$$

where $t_{exp}$ is the period over which exposure is computed.

#### *NAPL Source*

A NAPL source is modeled as a region between initial upper and lower depths with a specified average soil concentration of COC and total hydrocarbon. The COC is assumed to deplete over time because of volatilization, resulting in a decrease in the thickness of the COC contaminated zone over time. Mass loss from leaching is disregarded. The vapor concentration within the source is assumed to remain constant until the entire COC mass in the source is depleted. These are conservative assumptions because additional mass will be lost from leaching and because as the mole fraction of a volatile COC decreases over time, the equilibrium vapor concentration will diminish. Assuming furthermore that the COC vapor concentration at the soil surface (or soil-building interface) is much lower than the vapor concentration at the source, the rate at which the source zone thickness decreases may be estimated by

$$\frac{dL}{dt} = \frac{b D^{coc}_{eff} C^{coc}_{source}}{\rho S_{coc} L} \quad (3)$$

where b is a factor to account for the increase in COC diffusive flux from biodecay, (described later), $D^{coc}_{eff}$ is the effective vapor diffusion-dispersion coefficient for the COC (described later), $C^{coc}_{source}$ is the vapor concentration of the COC in equilibrium with NAPL at the source, $\rho$ is the soil bulk density, $S_{coc}$

is the mass of COC per mass of dry soil, and L is distance from the foundation to the top of the source. The depth to the top of the source at a specified time, t, may be estimated by integrating Equation 3 to yield

$$L_t = \frac{1}{b}\min\left( L_b \left( \frac{2bD^{coc} C^{coc}_{source} t}{\rho S_{coc}} + L_o^2 \right)^{1/2} \right) \quad (4)$$

where $L_o$ is the initial depth to the top of the source, $L_b$ is the depth to the bottom of the source, and $L_t$ is the current depth. The time to deplete COC from the entire NAPL source may be computed as

$$t_{max} = \frac{\rho S_{coc} b(L_b^2 - L_\infty^2)}{2D^{coc} C^{coc}_{source}} \quad (5)$$

The vapor concentration at the source is computed from Raoult's law as

$$C^{coc}_{source} = \frac{C^{coc}_{w*} H_{coc} S_{coc} M_{tph}}{S_{tph} M_{coc}} \quad (6)$$

where $C^{coc}_{w*}$ is the solubility of pure COC, $S_{tph}$ is the soil concentration of total hydrocarbons, $M_{coc}$ is the COC molecular weight, and $M_{tph}$ is the average molecular weight of the bulk NAPL.

### Soil Zone Model

The soil zone is the region between the upper boundary of the source zone and the building foundation. The model considers diffusion and dispersion driven by barometric pumping and biodecay, which may be limited by oxygen or other factors. Assuming negligible lateral diffusion, a mass balance over the region between the vapor source and the foundation (Figure 1) may be written as

$$J^{coc}_{net} = J^{coc}_{source} - B^{coc}_{bio} L_{coc} \quad (7)$$

where $J^{coc}_{net}$ is the mass of COC reaching the foundation per unit area per time, $J^{coc}_{source}$ is the mass of COC volatilizing from the source zone per unit area per time, $B^{coc}_{bio}$ is the average COC biodecay rate per unit soil volume, and $L_{coc}$ is the distance from the source (i.e., NAPL zone or capillary fringe) to the foundation. For a ground water source, $L_{coc}$ is constant over time, while it is updated with time via Equation 4 for a NAPL source.

#### *Diffusive-Dispersive Transport*

The volatilization flux from the source is computed assuming quasi-steady-state diffusion through the soil as

$$J^{coc}_{source} = \frac{bD^{coc}_{eff}(C^{coc}_{source} - C^{coc}_{soil})}{L_{coc}} \quad (8)$$

where $C^{coc}_{soil}$ is the vapor phase concentration of COC under the foundation, b is a factor to account for the increase in COC diffusive flux from biodecay (discussed later), and other variables are as defined previously. The effective diffusion-dispersion coefficient is estimated as

$$D^{coc}_{eff} = \bar{\tau} D^{coc}_o + A V_{bp} \quad (9)$$

where $\bar{\tau}$ is the effective tortuosity, $D^{coc}_o$ is the COC molecular diffusion coefficient in free air, A is the longitudinal dispersivity, and $V_{bp}$ is the mean air pore velocity magnitude from barometric pumping. Dispersivity is assumed to increase with travel distance from the source because of increases in heterogeneity with scale such that

$$A = \beta L_{coc} \quad (10)$$

where $\beta$ is the longitudinal dispersivity to travel distance ratio. The tortuosity in a given layer is estimated by

$$\tau = \phi_a^{3.33} \phi^{-2} \quad (11)$$

where $\phi$ is the total soil porosity and $\phi_a$ is the air-filled porosity (Millington and Quirk 1961; Jury et al. 1990; Johnson and Ettinger 1991; Jeng et al. 1996; Fischer et al. 1996). For a layered soil, the effective tortuosity may be computed as the weighted harmonic average of the layers (i.e., $\Sigma L_i / \Sigma L_i/\tau_i$).

For airflow induced by barometric pressure fluctuations, the Darcy velocity may be derived from the ideal gas law (Auer et al. 1996). For a periodic relative pressure fluctuation $p_{bp}$ (fluctuation range divided by mean pressure) with period $T_{bp}$, air in the soil will be compressed (or decompressed) by a relative amount $p_{bp}$ over a time interval $T_{bp}/2$. Therefore, the mean absolute Darcy velocity at the ground surface, $q^o_{bp}$, is given by

$$q^o_{bp} = \frac{2p_{bp} L_{bp} \bar{\phi}_a}{T_{bp}} \quad (12)$$

where $L_{bp}$ is the depth of barometric pressure propagation, $\bar{\phi}_a$ is the average air-filled porosity over all layers, and other terms are as previously defined. The depth-averaged velocity will be half that at the ground surface and the mean air pore velocity is equal to the Darcy velocity divided by $\bar{\phi}_a$, which yields

$$V_{bp} = \frac{p_{bp} L_{bp}}{T_{bp}} \quad (13)$$

The depth of barometric pressure propagation, $L_{bp}$, is taken as the lesser of the depth to ground water (or more accurately the capillary fringe) below ground ($L_{wt}$) or the maximum depth limited by the air permeability of the soil ($L_{perm}$). The latter is approximated by

$$L_{perm} = \frac{\bar{k}_{air} p_{bp} P_o T_{bp}}{2\bar{\phi}_a \mu_a} \quad (14)$$

where $\bar{k}_{air}$ the average intrinsic air permeability, $P_o$ is the mean atmospheric pressure, and $\mu_a$ is the dynamic air viscosity. The average air permeability may be computed as the weighted harmonic average of layer values (i.e., $\Sigma L_i/\Sigma L_i/k_i$) and average porosity may be computed as the weighted arithmetic mean of layers (i.e., $\Sigma L_i\phi_i/\Sigma L_i$).

For a NAPL source, the source depth in Equation 8 increases with time according to Equation 4, resulting in decreased COC volatilization rates over time. Average rates over time are determined by performing calculations at specified time intervals and averaging. For a dissolved ground water source, the source depth is regarded as a constant over time equal to the average depth from foundation to the top of the capillary fringe.

*Biodecay in Soil*

It is assumed that the biodecay rate per soil volume ($B^{bio}_{coc}$) is equal to the lesser of: (1) the maximum decay rate ($B_1$) when oxygen is nonlimiting (the "intrinsic" biodecay rate), (2) the rate limited by diffusive-dispersive oxygen transport from the soil surface or soil-building interface into the soil ($B_2$), or (3) the rate limited by oxygen from air flowing from the soil surface under the building ($B_3$). The maximum COC decay rate per area when oxygen is not limiting is estimated as

$$B_1 = R_{coc}\gamma_{max}\rho \tag{15}$$

where $R_{coc}$ is the proportion of the total biodecay attributable to the COC ("relative biodecay rate"), $\gamma_{max}$ is the maximum total hydrocarbon mass that can be degraded per day per unit soil mass, and $\rho$ is the soil bulk density. The biodecay rate limited by oxygen transport is

$$B_2 = \frac{FR_{coc}\, C^{ox}_{atm}\, D^{ox}_{eff}}{L_{nox}\, L_{coc}} \tag{16}$$

where $R_{coc}$ is the relative biodecay rate, F is a stoichiometric coefficient representing the total mass of hydrocarbon that may be degraded per unit mass of oxygen utilization, $D^{ox}_{eff}$ is the effective diffusion-dispersion coefficient for oxygen in the soil computed as in Equation 9 using the free air diffusion coefficient for oxygen, $C^{ox}_{atm}$ is the concentration of oxygen in the atmosphere (i.e., 274 mg/L), and $L_{nox}$ is the depth at which oxygen is depleted, computed as

$$L_{nox} = \min\left[L_{coc}\left(\frac{FD^{ox}_{eff}\, C^{ox}_{atm}}{\rho\gamma_{max}}\right)^{1/2}\right] \tag{17}$$

where the second term in brackets represents the depth at which $B_1 = B_2$. Finally, the biodecay rate may be limited by advective oxygen transport computed as

$$B_3 = \frac{FR_{coc}\, C^{ox}_{atm}\, (Q_{soil} + Q_{sub})}{A_e\, L_{coc}} \tag{18}$$

where $Q_{soil}$ and $Q_{sub}$ are the volumetric airflow rates from the soil surface into the building and under the foundation, respectively (discussed later), $A_e$ is the lesser of the source area or the building area, and other terms are as previously defined.

When biodecay occurs in the soil, the COC concentration gradient will not be constant with depth. The rate of COC volatilization at the source will be greater than that computed using the average gradient between the source and the foundation by a factor *b*. If biodecay is approximated by first-order kinetics, the gradient enhancement factor is (Cussler 1984, p. 350)

$$b = \frac{\tanh(L_{coc}(\gamma_{fo}/D^{coc}_{eff})^{1/2})}{L_{coc}(\gamma_{fo}/D^{coc}_{eff})^{1/2}} \tag{19}$$

where $\gamma_{fo}$ is an apparent first-order decay coefficient, which may be estimated considering a mass balance over the soil zone as

$$\gamma_{fo} = \frac{\ln\left(\frac{J^{coc}_{source}}{J^{coc}_{ner}}\right)}{\frac{L^2_{coc}}{D^{coc}_{eff}}} \tag{20}$$

where the numerator represents the relative mass loss between the source and the foundation, and the denominator is an approximation of the travel time. Note that Equations 19 and 20 are recursive because of the dependence of fluxes on *b*.

*Relative Biodecay Rates for Hydrocarbon Mixtures*

The total mass biodegraded aerobically within a given volume of soil per time is controlled in the model by the lesser of the oxygen availability or the intrinsic biodecay rate (e.g., as measured in an in situ respiration test). For multispecies contaminant mixtures, the total potential decay will be distributed among multiple species. The fraction of the total decay that is attributable to a specific COC is defined as the relative biodecay rate ($R_{coc}$ in Equations 15, 16, and 18). Uptake of organic chemicals for metabolism by microorganisms is generally understood to occur via the aqueous phase (Zhang et al. 1995). Therefore, the uptake rate of a given species will depend on its aqueous concentration and on any other chemical-specific factors that result in preferential uptake. Accordingly, we assume

$$R_{coc} = \frac{\text{uptake rate for COC}}{\text{total uptake rate for all species}} \tag{21a}$$

$$= \frac{\bar{C}^{w}_{coc}\, p_{coc}}{\sum_{i=1}^{N} \bar{C}^{w}_{i}\, p_i} \tag{21b}$$

where $\bar{C}^{w}_{i}$ is the average aqueous concentration of species *i* within the soil volume of interest, $p_i$ is a biopreference factor for uptake of species i, $\bar{C}^{w}_{coc}$, and $p_{coc}$ are respective quantities

**Table 1**
**Measured and Predicted Relative Biodecay Rates for McAllister et al. (1995) Data**

| Species | Relative Biodecay Rate | | |
|---|---|---|---|
| | Observed | Calculated $p = K_{oc}$ | Calculated $p = 1$ |
| Benzene | 0.03 | 0.03 | 0.39 |
| Toluene | 0.10 | 0.07 | 0.48 |
| *m*-xylene | 0.20 | 0.21 | 0.13 |
| *n*-pentane | 0.68 | 0.69 | 0.003 |

for the COC, and N is the total number of species (or pseudo-species) that may be aerobically degraded.

Chemicals with a higher affinity for organic matter may be expected to exhibit higher passive uptake rates by microorganisms at a given dissolved-phase concentration. Therefore, to the extent that uptake biopreference can be attributed to differences in passive uptake rates, the organic carbon partition coefficient for species *i*, $K_{oci}$, might be expected to serve as a first approximation of the biopreference factor, $p_i$.

Results of a laboratory study by McAllister et al. (1995) may be employed to evaluate the validity of Equation 21 and the characterization of $p_i$. The study involved a column experiment with a NAPL mixture that was leached with aerated water under saturated conditions. The NAPL comprised a 0.0025 mass fraction of benzene, 0.0125 toluene, 0.0125 *m*-xylene, and 0.9725 *n*-pentane. The quantity of each species removed in effluent and remaining in the column at the end of the experiment was determined, enabling direct calculation of biodecay rates of each species. Because dissolved-phase concentrations in this study will be controlled by mass transfer from the NAPL, the relative biodecay rate may be computed from Equation 21 as

$$R_{coc}^{sat} = \frac{m_{coc} C_{coc}^{sol} p_{coc}}{\sum_{i=1}^{N} m_i C_i^{sol} p_i} \tag{22}$$

where $R_{coc}^{sat}$ is the relative COC decay rate in ground water under conditions in which the dissolved phase concentration is controlled by dissolution from NAPL, $m_i$ is the mole fraction of species *i* in the NAPL, $C_i^{sol}$ is the solubility of pure species *i*, $p_i$ is the bioselectivity factor for species *i*, and variables with a subscript COC denote respective variables for the COC.

The actual relative biodecay rates computed directly from the experimental mass-balance data and those calculated from Equation 22 with $p_i = 1$ and $p_i = K_{oci}$ are compared in Table 1. It is evident that assuming no biopreference ($p_i = 1$) leads to substantial overestimation of biodecay for the more soluble aromatics and to underestimation for the less soluble alkanes. In contrast, $p_i = K_{oci}$ produces very close agreement with the data, reflecting the inverse correlation between solubility and $K_{oc}$. These results confirm the validity of Equation 21 and indicate the assumption that $p_i = K_{oci}$ is a reasonable approximation, at least for the hydrocarbons in this study.

For the vapor-phase transport model described in this paper, application of Equations 21 requires characterization of average dissolved-phase concentrations between the source zone and the foundation (the "soil zone"). The average dissolved-phase concentration of a given species in the soil zone will be proportional to the mass flux of the species into the soil zone times the fraction of the total mass of the species that partitions into the aqueous phase. Assuming the vapor concentration at the source is much greater than the vapor concentration at the ground surface, the mass flux of a given species into the soil zone will be proportional to the vapor-phase concentration at the source (Equation 8). Therefore, the average dissolved-phase concentration of a species in the soil zone will be proportional to the vapor concentration in the soil times the fraction of the species that partitions to the aqueous phase. Accordingly, Equation 21 may be written for the case of biodecay in the soil zone due to a volatile source as

$$R_{coc}^{vap} = \frac{f_{coc} C_{coc}^{vap} p_{coc}}{\sum_{i=1}^{N} f_i C_i^{vap} p_i} \tag{23}$$

where $R_{coc}^{vap}$ is relative COC decay rate in the soil zone under conditions in which the contaminant occurs because of volatilization from a source zone, $C_i^{vap}$ is the vapor concentration of species *i* at the source, $f_i$ is the fraction of the total mass of species *i* that partitions into the dissolved phase, $p_i$ is the bioselectivity factor for species *i*, and variables with subscript COC denote respective variables for the COC. Assuming equilibrium phase partitioning, $f_i$ may be computed by

$$f_i = \frac{\phi_w}{\phi_w + \phi_a H_i + \rho_b f_{oc} K_{oci}} \tag{24}$$

where $\phi_w$ is the volumetric water content, $\phi_a$ is the air-filled porosity, $H_i$ is Henry's constant for species *i*, $\rho_b$ is the soil bulk density, $f_{oc}$ is the organic carbon fraction of the soil, and $K_{oci}$ is the organic carbon partition coefficient for species *i*. Combining Equations 23 and 24 yields

$$R_{coc}^{vap} = \frac{C_{coc}^{vap} p_{coc} \sum_{i=1}^{N} (\phi_w + \phi_a H_i + \rho_b f_{oc} K_{oci})}{(\phi_w + \phi_a H_{coc} + \rho_b f_{oc} K_{oc}^{coc}) \sum_{i=1}^{N} C_i^{vap} p_i} \tag{25}$$

We will use Equation 25 to characterize relative biodecay rates for constituents volatilizing from a source in the unsaturated zone.

## Building Indoor Air Model

For vapor intrusion into a building, the model of Johnson and Ettinger (1991) for advective and diffusive transport through foundation cracks or other continuous pores is employed. The rate of COC intrusion into a building is given by

**Table 2**
Parameter Ranges for Example 1 Base Case and Contribution to the Variance in 30-Year Average Benzene Concentration in Indoor Air

| Parameter (Units) | Minimum Value | Maximum Value | Contribution to Variance (%) |
|---|---|---|---|
| Subbase air permeability ($m^2$) | $10^{-9}$ | $10^{-7}$ | 32.5 |
| Relative biodecay rate for COC (–) | 0.0006 | 0.06 | 25.8 |
| COC attenuation rate in ground water (yr) | 0.05 | 0.15 | 15.9 |
| Maximum total biodecay rate (mg/kg/day) | 1 | 10 | 10.5 |
| Air-filled porosity (–) | 0.28 | 0.32 | 3.7 |
| Building exchange rate (exchanges per hour) | 0.5 | 1.5 | 3.0 |
| Longitudinal dispersivity/travel distance ratio (–) | 0.005 | 0.08 | 2.1 |
| Subbase pressure differential (Pa) | 3 | 15 | 1.8 |
| Building depressurization (Pa) | 1 | 5 | 1.6 |
| COC source concentration (μg/L) | 4500 | 5500 | 1.2 |
| Soil air permeability ($m^2$) | $10^{-15}$ | $10^{-14}$ | 1.1 |
| Total porosity (–) | 0.38 | 0.42 | 0.7 |
| Barometric pressure range/period (atm/day) | 0.01 | 0.03 | 0.2 |
| Effective foundation porosity (–) | 0.001 | 0.01 | < 0.1 |

$$E = Q_{soil}C^{coc}_{soil} - \frac{Q_{soil}(C^{coc}_{soil} - C^{coc}_{bldg})}{1 - \exp(Q_{soil}L_{slab}/\eta D^{coc}_{o} A_b)} \quad (26)$$

where E is the mass of COC entering the building per time; $Q_{soil}$ is the volumetric flow rate of soil gas into the building; $C^{coc}_{soil}$ and $C^{coc}_{bldg}$ are vapor concentrations of COC immediately under the foundation and in the building, respectively; $L_{slab}$ is the foundation thickness; $D^{coc}_{o}$ is the diffusion coefficient for COC in free air; η is the effective porosity of the foundation that is permeable to air (a.k.a. fraction of foundation area with cracks), and $A_b$ is the building foundation area. The free air diffusion coefficient is used here as a conservative (i.e., high) estimate of the crack diffusion coefficient. The volumetric airflow from the ground surface into the building is computed following Johnson and Ettinger (1991) as

$$Q_{soil} = \frac{2\pi\Delta P_{bldg} k U K_{soil} X}{\mu \ln(2ZX/\pi A_b)} \quad (27)$$

where $\Delta P_{bldg}$ is the building depressurization, $k_{soil}$ is the air permeability of the soil between the ground surface and the foundation, X is the total building perimeter, μ is the air viscosity, Z is the foundation depth below grade, and other terms are as previously defined.

The foregoing equations may be solved for $C^{coc}_{bldg}$ noting that at (pseudo-) steady state the mass of COC entering the building per time (E) is given by

$$E = Q_{bldg} C^{coc}_{bldg} = J^{coc}_{net} A_e - Q_{sub}C^{coc}_{soil} - B_{sub} \quad (28)$$

where $Q_{bldg}$ is the total volumetric building air exchange rate (air volume in building times building volume changes per hour), $A_e$ is the lesser of the contaminated soil area under the building or the building foundation area, $Q_{sub}$ is the volumetric airflow rate under the building foundation from the upwind to leeward side of the building ("foundation cross-flow"), and $B_{sub}$ is the mass biodegraded per time in the subbase region under the foundation. The magnitude of $Q_{sub}$ that short-circuits vapor from beneath the building to the atmosphere is computed as

$$Q_{sub} = \frac{k_{avg}\Delta P_{sub} L_{sub} A_b^{1/2}}{\mu(A_b^{1/2} + 2Z)} \quad (29)$$

where $\Delta P_{sub}$ is the pressure drop in the outside air between the upwind and downwind side of the building, $L_{sub}$ is the thickness of the subbase material underlying the foundation, and $k_{avg}$ is the average (in-series) permeability along a path from the upwind to downwind sides of the building passing below the building calculated as

$$k_{avg} = \frac{A_b^{1/2} + 2Z}{\frac{A_b^{1/2}}{k_{sub}} + \frac{2Z}{k_{soil}}} \quad (30)$$

where $k_{sub}$ is the subbase permeability, $k_{soil}$ is the soil permeability, and Z is the foundation depth.

The subbase COC biodecay rate, $B_{sub}$, is computed as

$$B_{sub} = \text{Min}\left(\rho R_{coc}\gamma_{max} L_{sub} A_e, FR_{coc}C^{ox}_{atm}(Q_{sub} + Q_{soil}) - B^{coc}_{bio} L_{coc} A_e\right) \quad (31)$$

where all terms are as previously defined.

## Uncertainty in Exposure Concentrations and Risk Analysis

Because, in practice, model parameters are not exactly known, model results will also be subject to uncertainty. A first-order error analysis method is used to determine confidence limits on calculated vapor exposure concentrations (Unlu et al. 1995). For a given set of upper and lower estimates of model

Table 3
Comparison of Example 1 Base Case and Sensitivity Analysis Results

| Case | Mean Indoor Air Concentration ($\mu g/m^3$) | Baseline Risk | Ground Water Cleanup Level ($\mu g/L$) |
|---|---|---|---|
| Base Case | 6.8 | $1.7 \times 10^{-5}$ | 2300 |
| 1 – higher source concentration | 79.4 | $2.0 \times 10^{-4}$ | 2300 |
| 2 – finer grained soil | 0.001 | $3.0 \times 10^{-9}$ | 34,000 |
| 3 – slab on grade foundation | 0.16 | $4.1 \times 10^{-7}$ | 10,000 |
| 4 – no foundation cross-flow | 41.7 | $1.1 \times 10^{-4}$ | 900 |
| 5 – no source attenuation over time | 46.5 | $1.2 \times 10^{-4}$ | 800 |
| 6 – no barometric pumping | 4.8 | $1.2 \times 10^{-5}$ | 2350 |
| 7 – no biodecay | 19.0 | $4.9 \times 10^{-5}$ | 100 |

parameters (at a given probability level), mean exposure concentrations and upper and lower confidence limits are calculated for the same probability level as the input parameters. Log-normal probability distributions are assumed for model parameters and predicted exposure concentrations. For purposes of computing health risk, the mean exposure concentration is employed in all risk calculations. Excess carcinogenic risk or hazard quotient is computed for carcinogenic or chronic toxic chemicals, respectively, using standard protocols (ASTM 1995).

## Case Study 1: Volatilization from Ground Water

### Base Case Scenario

The first case involves volatilization from contaminated ground water under a hypothetical building with a basement in sandy soil. Ground water with benzene contamination occurs 4 m below ground surface. The current concentration of benzene is 5000 µg/L and monitoring indicates a downtrend of ~10% per year. The building is 10 × 20 m with an air volume of 600 $m^3$ and the foundation is 2 m below grade underlain by a 0.1 m thick gravel subbase. The average indoor air concentration is computed over an exposure period of 30 years, and health risk is calculated for an average adult for residential exposure.

Upper and lower estimates of model parameters for the base case are given in Table 2. Parameter ranges represent typical uncertainty in parameter estimates at gasoline spill sites. The relative biodecay rate for benzene with co-contaminants from gasoline was computed from Equation 25 using $p = K_{oc}$. Gasoline composition was approximated by a 36-species mixture. The resulting benzene relative biodecay rate for gasoline volatilizing into the unsaturated zone was estimated to be 0.006, which was assumed to be accurate within a factor of 10 (i.e., 0.06 to 0.0006). Free air molecular diffusion coefficient for benzene and oxygen were taken as 0.75 and 1.18 $m^2$/day, respectively. The dispersivity-travel distance ratio, β, was assumed to be between 0.005 to 0.08, which brackets the median value of ~0.02 indicated by studies of aqueous phase transport in the unsaturated zone (Gelhar et al. 1985). Because hydrodynamic dispersion is primarily controlled by large-scale heterogeneity rather than pore geometry, it is reasonable to assume vapor dispersivity is similar to that for aqueous transport for analogous conditions (i.e., vertical transport in the unsaturated zone), although field studies are needed to assess this further.

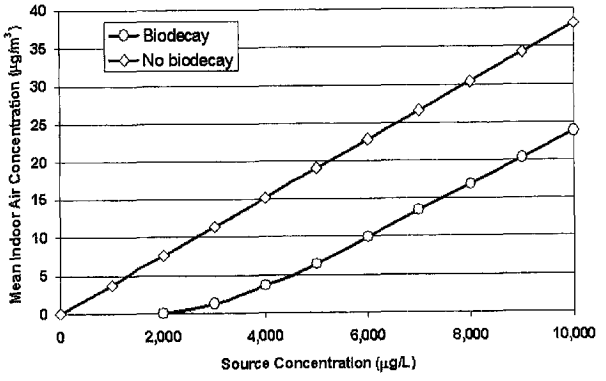


Figure 2. Predicted indoor air concentrations with and without biodecay.

The 30-year average benzene concentration in indoor air was calculated to have lower and upper estimates of 0.4 to 33 µg/$m^3$ with a mean value of 6.8 µg/$m^3$, yielding a baseline risk of $1.7 \times 10^{-5}$. For a target risk of $10^{-6}$, the ground water cleanup level for benzene was calculated to be 2300 µg/L, assuming exposure is caused solely by inhalation of indoor air (Table 3).

Contributions to the model variance are summarized for all uncertain model parameters in Table 2. Uncertainty in subbase air permeability and COC relative biodecay rate, and to a lesser extent COC attenuation rate in ground water and the total biodecay rate, account for nearly 85% of the uncertainty in the benzene concentration in indoor air for this problem.

## Sensitivity Analyses

Predicted mean indoor air concentrations, baseline risk, and risk-based cleanup levels for benzene in ground water are summarized in Table 3 for the sensitivity analyses. The risk-based cleanup level for benzene in ground water for the base case was 2300 µg/L. Increasing the source concentration by a factor of 5 (case 1) increased the mean indoor air concentration by a factor of 12.5.

This disproportionate increase in indoor air concentration reflects the nonlinear effects of biodecay on exposure lev-

Table 4
Parameter Ranges for Base Case and NAPL Source Secenario and Contributions to the Variance in 30-Year Average Benzene Concentration in Indoor Air

| Parameter (Units) | Minimum Value | Maximum Value | Contribution to Variance (%) |
|---|---|---|---|
| Subbase air permeability ($m^2$) | $10^{-9}$ | $10^{-7}$ | 54.4 |
| Soil air permeability ($m^2$) | $10^{-12}$ | $10^{-11}$ | 15.1 |
| Building depressurization (Pa) | 1 | 5 | 7.2 |
| Subbase pressure differential (Pa) | 3 | 15 | 7.2 |
| Relative biodecay rate for COC (–) | 0.0006 | 0.06 | 5.8 |
| Building exchange rate (exchanges per hour) | 0.5 | 1.5 | 5.0 |
| COC source conentration (mg/kg) | 50 | 100 | 3.1 |
| NAPL source TPH concentration (mg/kg) | 2500 | 10,000 | 1.6 |
| Effective foundation porosity (–) | 0.001 | 0.01 | 1.0 |
| Maximum total biodecay rate (mg/kg/day) | 1 | 10 | 0.4 |
| Air-filled porosity (–) | 0.28 | 0.32 | 0.2 |
| Longitudinal dispersivity/travel distance ratio (–) | 0.005 | 0.08 | <0.1 |
| Barometric pressure range/period (atm/day) | 0.01 | 0.03 | <0.1 |
| Total porosity (–) | 0.38 | 0.42 | <0.1 |

els. As source concentration increases, the volatilization rate increases, whereas biodecay remains essentially constant, leading to a disproportionate increase in indoor air emissions. An analysis of variance for case 1 indicates that the relative biodecay rate accounts for only 8% of the uncertainty (compared with 26% for the base case), which further confirms the foregoing explanation.

Decreasing soil permeability and air-filled porosity (case 2) was predicted to decrease indoor air concentrations and baseline risk to negligible levels and to increase the risk-based ground water cleanup level close to the effective solubility of benzene from gasoline, indicating there is very little possibility of adverse exposure (via the assumed pathway) for this scenario.

Changing from a basement to slab on grade (case 3) resulted in lower indoor air concentrations and risk and, as a result, higher cleanup levels. The shallow foundation exhibits less air intrusion from the soil to the building and greater foundation cross-flow, which reduce indoor air concentrations. Disregarding foundation cross-flow and source attenuation over time (cases 4 and 5), as is common in most screening models, led to substantial overestimation of indoor air concentration and risk and to underestimation of cleanup level. For the specific conditions of the example, indoor air concentrations and risk increased by about seven times relative to the base case, and risk-based cleanup levels decreased by a factor of ~3 for these cases.

Barometric pumping had little effect on the model results (case 6). Disregarding barometric pumping decreased predicted indoor air concentration and risk and increased the cleanup level by small amounts relative to the base case. Fluxes from barometric pumping will be greater relative to diffusive fluxes for conditions with low air-filled porosity and/or large depth to ground water. However, barometric fluctuations concurrently increase contaminant volatilization and oxygen transport, which tend to have opposing effects on indoor air.

Disregarding biodecay entirely (case 7) resulted in overestimation of indoor air concentrations and risk by a factor of ~3 and to underestimation of cleanup level by a factor of 23 in comparison with the base case. In the absence of decay, indoor air concentration is a linear function of source concentration. Biodecay results in a threshold source concentration, below which no emissions occur because the potential decay rate exceeds the rate of source volatilization (Figure 2). Note that the two curves in Figure 2 converge slightly at lower source concentrations because of enhanced diffusive gradients caused by biodecay (i.e., the factor $b$ in Equation 8 increases as source concentration decreases).

This threshold effect has an important influence on the calculation of risk-based cleanup levels. Without biodecay, the baseline risk to target risk ratio (BTR) is equal to the ratio of current source concentration-to-cleanup level (SCR). As expected, for case 7 BTR/SCR = 1. For other cases, ratios as high as 55 are observed, reflecting the nonlinearity of the risk-cleanup response when biodecay is considered. Risk-based cleanup levels are much lower when biodecay is considered. Conversely, actual risk may be much lower than the calculated risk if biodecay is disregarded, even if biodecay rates are small. Note that in the present example, <1% of the available oxygen is consumed by benzene biodecay.

It is interesting to compare the present modeling approach for biodecay with a simple first-order biodecay model. Equation 20 yields an apparent first-order decay coefficient for the base case of 0.028 $d^{-1}$. Case 1, which is identical except for a higher source concentration, yields an apparent first-order rate coefficient of only 0.0045 $d^{-1}$. The lower coefficient reflects an increase in source volatilization, whereas biodecay remains constant because of the limited oxygen supply. Due to the dependence of apparent first-order rate coefficients on many system variables, extrapolation of rate coefficients to conditions different from those for which they were measured may lead to large errors.

Table 5
Comparison of Example 2 Base Case and Sensitivity Analysis Results

| Case | Mean Indoor Air Concentration ($\mu g/m^3$) | Baseline Risk |
|---|---|---|
| Base Case | 12.6 | $3.2 \times 10^{-5}$ |
| 1 – finer gained soil | 0.04 | $9.5 \times 10^{-8}$ |
| 2 – increase foundation depth | 14.0 | $3.6 \times 10^{-5}$ |
| 3 – increase source and ground water depth | 5.1 | $1.3 \times 10^{-5}$ |
| 4 – decrease soil COC and TPH | 2.5 | $6.5 \times 10^{-6}$ |
| 5 – decrease soil COC only | 0.02 | $4.0 \times 10^{-8}$ |
| 6 – no foundation cross-flow | 70.5 | $1.8 \times 10^{-4}$ |
| 7 – no source depletion | 859.0 | $2.9 \times 10^{-3}$ |
| 8 – no barometric pumping | 13.0 | $3.3 \times 10^{-5}$ |
| 9 – no biodecay | 16.3 | $4.2 \times 10^{-5}$ |

## Case Study 2: Volatilization from a NAPL Source

### Base Case Scenario

The second example involves residual gasoline in a sandy soil. The base case scenario considers a slab-on-grade building with a 0.1 m thick gravel subbase under the floor slab. A NAPL-contaminated zone is present from 5 to 6 m below ground surface with an average soil TPH concentration of 5000 mg/kg and an average soil benzene concentration of 75 mg/kg, corresponding to an initial benzene mass fraction of 1.5%. The water table occurs at a depth of 6 m. The building is 10 × 20 m with an air volume of 600 $m^3$. The average indoor air concentration is computed over an exposure period of 30 years and health risk is calculated for an average adult for residential exposure.

A summary of assumed upper and lower estimates of parameters for the base case scenario is given in Table 4. The relative biodecay rate for benzene with co-contaminants from gasoline was computed as for case study 1, yielding a mean relative biodecay rate of 0.006. Henry's constant for benzene is 0.18 and the solubility is 1870 mg/L. The 30-year average benzene concentration in indoor air was calculated to have a mean value of 12.6 $\mu g/m^3$ with lower and upper estimates of 1 to 53 $\mu g/m^3$. Contributions to the model variance computed from the first-order error analysis are summarized for all uncertain model parameters in Table 4. The results indicate that uncertainty in subbase and soil air permeability together account for nearly 70% of the uncertainty in predicted benzene concentration in indoor air for this problem. Uncertainty in relative biocecay rate accounted for only 5% of the variance.

The mean indoor air concentration yields a baseline risk of $3.2 \times 10^{-5}$. Assuming a target risk of $10^{-6}$ and little change in the soil TPH concentration, the soil cleanup level for benzene was calculated to be 17 mg/kg. If soil TPH concentration is assumed to decrease proportionately with removal of benzene, a benzene cleanup level of 0.3 mg/kg is computed. The higher cleanup level for the former case reflects the decrease in equilibrium vapor pressure from lower mole fractions of benzene in the NAPL. The "true" cleanup level will generally lie between these two values and will depend on the specific reduction in TPH concentration that occurs concomitant with benzene reduction. For example, if soil vapor extraction is used, how much benzene is extracted compared with other hydrocarbon species. The results clearly demonstrate that soil cleanup levels for COCs in NAPLs cannot be defined independently of the total hydrocarbon concentration. That this must be so should be readily apparent because the COC mass fraction in the NAPL, rather than the COC soil concentration, controls the soil vapor concentration and hence emission rate.

### Sensitivity Analyses

Sensitivity analyses were performed with specified parameter adjustments from the base case values. The following scenarios were analyzed:

1. Silty soil with air permeability 1% of sandy soil and air-filled porosity of 0.1.
2. Increase foundation depth to 1.5 m below grade.
3. Source depth and water table 10 m deeper than base case.
4. Initial COC and TPH soil concentrations 10% of base case.
5. Initial COC soil concentration 10% of base case with TPH concentration unchanged.
6. No foundation cross-flow.
7. No source depletion over time.
8. No barometric pumping.
9. No biodecay.

Predicted mean indoor air concentrations and baseline risk for the base case and sensitivity analyses are summarized in Table 5. Cleanup levels were computed assuming TPH soil concentration is not decreased by remediation. Soil type had the greatest impact on the results, with results for the finer-grained soil (case 1) indicating low indoor air concentration and risk $<10^{-6}$.

Increasing foundation depth (case 2) and source depth (case 3) had minor effects on indoor air concentrations for the conditions studied. Decreasing COC and TPH concentrations simultaneously by a factor of 10 (case 4) resulted in indoor air decreasing by five times. Decreasing COC concentration by a factor of 10 with TPH concentration unchanged (case 5) was predicted to decrease average indoor air concentration over the 30-year exposure period by a factor of >500. Such a case may occur if product composition corresponded to a diesel-like hydrocarbon rather than gasoline. These cases emphasize the importance of considering joint effects of soil COC and TPH levels on emissions when attempting to define soil cleanup levels.

Ignoring foundation cross-flow or underestimating the subbase permeability (case 6) was predicted to cause a large increase in concentration from reduced lateral flushing for the slab-on-grade structure. Disregarding COC source depletion with time (case 7) resulted in a more than 50-fold increase in the predicted 30-year average concentration in indoor air and a proportionate increase in health risk. These results indicate that commonly used indoor air screening models predicated on steady-state volatilization from a nondepleting source may greatly overestimate exposure.

Disregarding barometric pumping (case 8) had little effect on the predicted indoor air concentration for the conditions investigated. As discussed earlier, barometric pumping is expected to have a somewhat greater impact when air-filled porosity is low (hence low molecular diffusion) and/or when the water table is deeper (hence higher air velocities). Disregarding biodecay (case 9) had a minor impact on predicted vapor concentrations for this problem. When the magnitude of biodecay

**Table 6**
Estimated Relative Biodecay Rates for New Jersey Site

| Species | Relative Biodecay Rate "Observed" (Equation 43) | Relative Biodecay Rate Predicted (Equation 42) |
|---|---|---|
| Benzene | 0.0048 | 0.0009 |
| Toluene | 0.0088 | 0.0042 |
| Ethylbenzene | 0.0004 | 0.0006 |
| Xylenes | 0.0130 | 0.0029 |

is small compared to the volatilization flux from the source, low sensitivity to biodecay is expected. However, biodecay is expected to strongly affect computed cleanup levels due to the threshold effect discussed in the preceding section.

## Case Study 3: Building with Basement in New Jersey

### Site Description and Parameter Estimates

This case involves a building near a former petroleum distribution facility in Paulsboro, New Jersey. Soils at the site are primarily fine- to medium-grain sand with small fractions of silt and coarse sand. Ground water occurs at a depth of ~6 m below land surface. Site investigations have been conducted to determine hydrocarbon concentrations at various depths in soil samples, in soil vapor, in ground water, and in indoor air (Integrated Science & Technology 1997a, 1997b). Data from the site were used to predict indoor air concentrations of benzene, toluene, ethylbenzene, and xylenes (BTEX) for comparison to measured values.

#### *Source Parameters*

Average COC concentrations in ground water were specified to define the source. Measured dissolved concentrations and concentrations calculated from soil vapor measurements just above the water table via Henry's law indicated 95% confidence limits for mean dissolved COC concentrations of ~2200 to 5400 µg/L for benzene, 4900 to 11,000 µg/L for toluene, 700 to 1200 µg/L for ethylbenzene, and 3400 to 6400 µg/L for xylenes. Ground water depth was 6 m. Henry's constants for BTEX were taken as 0.18, 0.22, 0.23, and 0.19, respectively.

#### *Soil Parameters*

No major changes in lithology were reported with depth at the site. Based on measurements of core samples, 95% confidence limits for the average total porosity were 0.38 to 0.42 and those for air-filled porosity were 0.22 to 0.26. Soil bulk density was estimated to be 1550 to 1650 kg/m$^3$. Air permeability was estimated to be $10^{-12}$ to $10^{-11}$ m$^2$ based on grain size data. Effective diffusion coefficients for BTEX and oxygen were computed from measured total and air-filled porosity values.

#### *Barometric Pumping*

The relative barometric pressure range for the site was estimated from hourly observations at a nearby airport, which indicated average barometric pressure fluctuations of 0.01 to 0.03 atm/day. Longitudinal dispersivity was assumed to be 0.005 to 0.08 times the source depth.

**Table 7**
Observed and Predicted Indoor Air Concentrations (µg/m$^3$) for Case Study 3

| Species | Observed | Model Predictions Minimum | Mean | Maximum |
|---|---|---|---|---|
| Benzene | 2 | 0.6 | 13 | 63 |
| Toluene | 8 | 1.0 | 22 | 112 |
| Ethylbenzene | 3 | 0.1 | 2 | 12 |
| Xylenes | 17 | 0.3 | 8 | 44 |

#### *Biodecay Rate*

The maximum biodecay rate was assumed to range between 1 and 10 mg/kg/day and the stoichiometric ratio for biodecay was assumed to range from 0.3 to 0.4; these are consistent with other studies (Hinchee et al. 1992; Rifai et al. 1987). Theoretical biodecay rates were computed from Equation 31 using measured BTEX and TPH vapor concentrations above the water table. Literature values for $K_{oc}^{coc}$ and $H_{coc}$ were employed for COCs, and was $f_{oc}$ assumed to be 0.001. For typical weathered gasoline, $H_{tph}$ was estimated to be ~5 and $K_{oc}^{tph}$ was estimated to be ~500 cm$^3$/g

The accuracy of relative biodecay rates computed using Equation 25 was evaluated by performing a mass balance for the COCs and TPH between the water table and the soil surface using field data. Assuming biodecay is the only sink at steady-state and considering equilibrium phase partitioning, mass-balance requirements indicate that the relative biodecay rate is given by

$$R_{coc}^{observed} = \frac{\Delta C_a^{coc} H_{tph}(\phi_w + \phi_a H_{coc} + \rho_b f_{oc} K_{oc}^{coc})}{\Delta C_a^{tph} H_{coc}(\phi_w + \phi_a H_{tph} + \rho_b f_{oc} K_{oc}^{tph})} \quad (32)$$

where $\Delta C_a^{coc}$ and $\Delta C_a^{TPH}$ are the differences in vapor-phase concentrations between the source and the soil surface for COC or TPH, respectively, and other terms are as previously defined. Concentration changes were determined from measured BTEX and TPH vapor concentrations between the shallowest and deepest monitoring depths.

Predicted relative BTEX biodecay rates calculated from Equation 25, which is based on $K_{oc}$ as the biopreference factor, and "observed" relative biodecay rates determined from a mass-balance analysis of site data via Equation 32 are compared in Table 6. Both estimates indicate that BTEX decay accounts for < 2% of total oxygen utilization. Relative biodecay rates estimated from Equation 25 agree with values computed from the mass balance within a factor of ~5. Model simulations were performed using estimates from Equation 25 with upper and lower limits specified within a factor of 10 to assess the accuracy of calculations made with normally available data.

#### *Building Parameters*

The building at the site was ~4.0 × 9.75 m with an area of 39 m$^2$ and an interior volume of ~82 m$^3$. The basement floor

Table 8
Vapor and Dissolved Phase Concentrations at Water Table and Species Coefficients for COCs in California Site

| Species | Vapor Concentration (mg/L) | Dissolved Concentration (mg/L) | Henry's Coefficient (–) | $K_{oc}$ (L/kg) | Relative Biodecay Rate (–) |
|---|---|---|---|---|---|
| Benzene | 8 | 44 | 0.18 | 83 | 0.008 |
| Toluene | 8 | 36 | 0.22 | 295 | 0.011 |
| Isopentane | 140 | 2.9 | 49 | 1065 | 0.065 |
| *n*-pentane | 53 | 1.2 | 43 | 1215 | 0.029 |
| 2-methylpentane | 79 | 1.5 | 54 | 2910 | 0.064 |

was 1.5 m below grade. A floor thickness of 0.15 m was assumed and the footers were assumed to be 0.15 m below the bottom of the floor slab. Effective foundation porosity (a.k.a. fraction of cracks) was assumed to range between 0.001 to 0.01, following Johnson and Ettinger (1991). A typical residential building air exchange rate of 0.5 to 1.5 volume changes per hour was assumed. Building underpressure was assumed to range from 1 to 5 Pa and the subbase pressure differential was assumed to be between 3 to 15 Pa. These values are consistent with airflow driven by wind-induced pressure differentials (Fischer et al. 1996). A foundation subbase of 0.05 to 0.15 m thickness with a permeability of $10^{-9}$ to $10^{-7}$ $m^2$ was assumed.

## Model Results

A comparison of measured indoor air concentrations with predicted minimum, mean, and maximum estimates is given in Table 7. Measured concentrations fall within the range of predicted concentrations for all species and are within a factor of 0.2 to 3.4 times the predicted mean concentrations.

The upper and lower estimates of indoor air concentration differ by a factor of ~100 to 300, which reflects the effects of estimated uncertainty in model parameters. An analysis of variance was performed to assess the contribution of various parameters to the uncertainty in indoor air concentration. Subbase air permeability had the highest contribution, ranging from 26% to 62% of the total variance for the different species. Longitudinal dispersivity accounted for 8% to 27% of the variance, the relative biodecay factor accounted for 4% to 18% of the variance, and foundation pressure differential accounted for 2% to 5%. Soil air permeability, maximum total biodecay rate, and building underpressure accounted for <1% to 7% of the total variance. The foregoing variance contributions reflect parameter sensitivities for the specific conditions studied. Different parameter sensitivities may be expected for different conditions.

Baseline risk was calculated to be $3.2 \times 10^{-5}$ for benzene inhalation, assuming no change in source concentration over a 30-year exposure period. If natural and/or engineered attenuation caused the source concentration to decrease at a rate of 10% per year or greater, baseline risk for the exposure period drops below $10^{-6}$. To achieve a target risk of $10^{-6}$ with a constant source concentration over time, the cleanup level for benzene in ground water under the building was calculated to be 750 µg/L, which may be compared with the current average observed concentration of 3500 µg/L. Using the same model parameters, except disregarding decay, the mean indoor air concentration for benzene was computed to be 18 µg/$m^3$ with a baseline risk of $4.6 \times 10^{-5}$. These values are 1.4 times greater than those computed considering decay. To achieve a target risk of $10^{-6}$, the cleanup level for benzene in ground water with no decay and no source attenuation over time was calculated to be 75 µg/L, which is 10 times lower than the risk-based cleanup level computed without source attenuation but with decay considered. Thus, the increase in risk-based cleanup level caused by decay is disproportionately greater than the decrease in indoor air concentration and baseline risk caused by decay. The nonlinear relation between risk exceedance and risk-based cleanup levels reflects the fact that decay rate is not proportional to vapor concentration except at very low volatilization rates as discussed in Case Study 1.

Comparison of the calculated ground water cleanup level of 750 µg/L with the value of 50 µg/L estimated following ASTM Tier 1 protocols (ASTM 1995) reflects on the conservative nature of the latter protocol.

## Case Study 4: Slab on Grade Building in California

### Site Description and Parameter Estimates

The last case involves a gasoline leak from a service station in California reported by Fischer at el. (1996). Soils at the site consist of fine-grained fill with ground water at a depth of ~2 m. Vapor concentrations for several species were measured by Fischer et al. at various depths in the soil under the building and in areas surrounding the building, in outdoor and indoor air, and for headspace from ground water samples. Measurements of soil porosity, water content, soil permeability, and potential biodecay were also performed. Information was reported on building air turnover, airflow rates from the soil to the building, and building construction. Measured indoor air concentrations of benzene, toluene, isopentane, *n*-pentane, and 2-methylpentane reported by Fischer et al. (1996) were predicted and compared to measured values.

#### *Source Parameters*

Equilibrium vapor concentrations at the water table were specified to define the source based on ground water headspace measurements from single samples as reported by Fischer et al. (1996). Measured values were assumed to be uncertain within a factor of 0.67 to 1.5. Measured vapor concentrations, calculated equilibrium dissolved concentrations, Henry's coefficients, and $K_{oc}$ values are summarized in Table

**Table 9**
Properties of Soil Layers Used in Model for California Site

| Layer Depth (m) | Total Porosity | Air-Filled Porosity |
|---|---|---|
| 0.0 – 0.6 | 0.37 | 0.22 |
| 0.6 – 0.8 | 0.36 | 0.17 |
| 0.8 – 1.8 | 0.41 | 0.24 |
| 1.8 – 2.0 | 0.51 | 0.08 |

8. At the time that vapor concentrations were measured, the ground water depth was ~2 m.

*Soil Parameters*

Due to observed variations in total and air-filled porosity with depth from soil core measurements, four soil layers were defined in the model (Table 9). Soil bulk density was estimated to be between 1480 to 1610 kg/m$^3$. Effective diffusion coefficients for COCs and oxygen for the multilayer system were computed from species free air diffusion coefficients and layer porosities. Airflow tests at the site reported by Fischer et al. indicated soil air permeability between $10^{-12}$ and $10^{-11}$ m$^2$. The average measured soil organic carbon content was 0.0024.

*Barometric Pumping*

No direct measurements on the magnitude of barometric pressure fluctuations were available for the site. The amplitude of barometric pressure fluctuations was assumed to be between 0.01 to 0.03 atm/day. Longitudinal dispersivity was assumed to be 0.005 to 0.08 times the depth to ground water based on data in Gelhar et al. (1985).

*Biodecay Rate*

Estimates of the maximum biodecay rate were obtained from measurements of isopentane decay in laboratory microcosms. Data reported from experiments on two soil samples, after converting to a soil mass basis, indicate rates of 2.8 to 6.5 mg/kg/day. These values were specified as lower and upper limits of the maximum total biodecay rate, respectively. The stoichiometric ratio for biodecay was assumed to range from 0.3 to 0.4. Relative COC biodecay rates were estimated using Equation 25. Measurements of total volatile hydrocarbons were not available. However, measured vapor concentrations corresponded closely with vapor in equilibrium with slightly weathered gasoline, which is expected to exhibit a total vapor concentration of ~1000 mg/L. This value was used in Equation 25. Furthermore, $H_{tph}$ was estimated to be 5 and $K_{oc}^{tph}$ was estimated to be 500 L/kg, corresponding to somewhat weathered gasoline. Calculated relative COC biodecay rates are summarized in Table 8. The values range from 0.008 for benzene to 0.065 for isopentane. Simulations were performed using tabulated estimates with upper and lower limits specified within a factor of 10.

*Building Parameters*

The building at the site was ~5.5 × 9.1 m with an area of 50 m$^2$ and an interior volume of 120 m$^3$. The building was slab-on-grade construction. The slab thickness was reported to be 0.1 m and the slab depth below ground surface was assumed to be the same. Effective foundation porosity (a.k.a. fraction of "cracks") was assumed to range between 0.001 to 0.01. Direct measurements of building airflow by Fischer et al. (1996) indicated rates between 3000 to 9000 m$^3$/day with building depressurization of 1 to 5 Pa. These flow rates represent 1 to 3 air exchanges per hour. Based on subgrade-to-indoor air dilution for COCs and tracers tests, the flow rate entering the building from the soil was estimated by Fischer at al. (1996) to be 1 to 3 m$^3$/day. A foundation subbase of 0.1 to 0.15 m thickness was assumed with a permeability of $10^{-9}$ to $10^{-7}$ m$^2$ corresponding to gravel. For wind-induced pressure gradients, the outside pressure differential between the upwind and downwind side of a building is typically approximately three times greater than the induced building underpressure. Therefore, the subbase pressure differential was estimated to be between 3 and 15 Pa.

**Table 10**
Observed and Predicted Indoor Air Concentrations (μg/m) for California Site

| Species | Observed | Model Predictions Minimum | Mean | Maximum |
|---|---|---|---|---|
| Benzene | 2.9 | 0.3 | 7.4 | 40 |
| Toluene | 5.7 | 0.1 | 4.2 | 24 |
| Isopentane | 37.0 | 8.6 | 212 | 1115 |
| *n*-pentane | 5.1 | 3.0 | 75 | 398 |
| 2-methylpentane | 6.6 | 3.5 | 91 | 483 |

## Model Results

A comparison of measured indoor air concentrations with predicted minimum, mean, and maximum estimates is provided in Table 10. Although measured concentrations are within the range of predicted concentrations for all species, the model generally overpredicted mean concentrations, indicating a conservative bias by the model for this site.

Uncertainty in model parameters resulted in upper and lower estimates of indoor air concentration that differ by a factor of ~150. An analysis of variance was performed to assess the contribution of various parameters to uncertainty in indoor air concentration. Subbase air permeability had the highest contribution, ranging from 49% of the total variance for toluene to 77% for isopentane. Increasing subbase permeability will result in greater flushing of volatile COCs from under the building, and hence decreases concentrations in intruding air. Longitudinal dispersivity and relative biodecay rate accounted for 3% to 17% of the variance. Foundation pressure differential, building underpressure, source concentration, and building air exchange rate each accounted for 1% to 9% of the variance, and other parameters accounted for <1% each.

The sensitivity results suggest that the most probable cause of the overprediction of indoor air concentrations is underestimation of subbase air permeability, which leads to underestimation of subbase flushing associated with pressure differentials across the outside of the building. Due to the slab-on-grade construction, this phenomenon is predicted to be a major factor controlling vapor intrusion into the building.

The possibility was considered that soil permeability may be lower than estimated. If so, the amount of contaminated air

entering the building would be overestimated by the model resulting in overestimation of indoor air concentrations. Tracer tests and other investigations at the site by Fischer et al. (1996) indicated that the rate of air intrusion into the building ($Q_{soil}$) was between 1 and 3 $m^3$/day. Employing median values of soil permeability, building underpressure, and other parameters in Equation 27 yielded an air intrusion rate of 1.55 $m^3$/day, which agrees well with the direct measurements. It was therefore concluded that the model formulation and parameters accurately predict air intrusion rate and are not likely causes of model bias.

In the foregoing analysis, the effective diffusion coefficient was calculated as an in-series weighted average of several soil layers. The effects of assuming a homogeneous soil characterized by simple arithmetic average total and air-filled porosities was also investigated. The homogeneous case yielded indoor air concentrations nearly 10 times greater than the layered case, reflecting the effects of layers with low air-filled porosity at depths of ~0.6 to 0.8 m and 1.8 to 2.0 m. This emphasizes the potential importance of thin layers with low air-filled porosity on vapor transport through soil.

Fischer et al. (1996) observed sharp increases in vapor concentration gradients above a depth of ~0.6 m below ground surface that they attributed to a low diffusivity layer at this depth. An additional factor that may contribute to the observed gradient increase is a change in biodecay rate with depth. At a certain depth below the foundation (or ground surface), oxygen entering the soil may become depleted by biological activity in the soil. This depth may be computed from Equation 17, which indicates a value of 0.8 m using median parameter estimates. This is close to the depth at which the gradient changes markedly, suggesting the higher concentration gradient at shallow depths may reflect higher biodecay rates at this depth.

Baseline risk was calculated to be $1.9 \times 10^{-5}$ for benzene exposure from indoor air inhalation. If the target risk is $10^{-6}$, the cleanup level for benzene in ground water under the building was calculated to be 10,500 µg/L assuming no source attenuation over time. The measured average concentration at the water table was ~44,000 µg/L. Natural attenuation of the source of 15% per year or greater would bring the risk below the target level over a 30-year exposure period. If biodecay and source attenuation over time were disregarded, the risk-based cleanup level was calculated to be 1100 µg/L—much lower than the value computed considering biodecay. As previously noted, although biodecay rates may be very small (<1% of the available oxygen is consumed degrading benzene), biodecay can nevertheless have a significant effect on risk-based cleanup levels.

## Acknowledgment

This research was performed at Oak Ridge National Laboratory (ORNL) sponsored by the Laboratory Director's Research and Development Fund. ORNL is managed by UT-Battelle, LLC, for the U.S. Department of Energy under contract DE-AC05-00OR22725.

## References

American Society for Testing Materials. 1995. ASTM E-1739, Appendix X.2: *Emergency Standard Guide for Risk-Based Corrective Action Applied to Petroleum Release Sites*. Philadelphia, Pennsylvania: ASTM.

Auer, L.H., N.D. Rosenberg, K.H. Birdsell, and E.M. Whitney. 1996. The effects of barometric pumping on contaminant transport. *Journal of Contaminant Hydrology* 24, 145–166.

Borden, R.C., and P.B. Bedient. 1986. Transport of dissolved hydrocarbons influenced by oxygen-limited biodegradation. *Water Resources Research* 20, 225–232.

Camp Dresser & McKee. 1986. Investigation, analyses, and numerical simulation of subsurface vapor transport. Report to Office of USTs, U.S. EPA (contract no. 68-01-6939). Cambridge, Massachusetts: CDM.

Clements,W.E., and M.H. Wilkening. 1974. Atmospheric pressure effects on 222Rn transport across the earth-air interface. *Journal of Geophysical Research* 79, 5025–5029.

Cussler, E.L. 1984. *Diffusion–Mass Transfer in Fluid Systems*. Cambridge, Massachusetts: Cambridge University Press.

Fischer, M.L., A.J. Bentley, K.A. Dunkin, A.T. Hodgson, W.W. Nazaroff, R.G. Sextro, and J.M. Daisey. 1996. Factors affecting indoor air concentrations of volatile organic compounds at a site of subsurface gasoline contamination. *Environmental Science & Technology* 30, 2948–2957.

Gelhar, L.W., A. Mantoglou, C. Welty, and K.R. Rehfeldt. 1985. A review of field-scale physical solute transport processes in saturated and unsaturated media. Electric Power Research Institute Research Project 2485-5.

Hers, I., J Atwater, L. Li, and R. Zapf-Gilje. 2000. Evaluation of vadose zone biodegradation of BTX vapours. *Journal of Contaminant Hydrology* 46, 233–264.

Hinchee, R.E., S.K. Ong, R.N. Miller, D.C. Downey, and R. Frandt. 1992. *Test Plan and Technical Protocol for a Field Treatability Test for Bioventing*. San Antonio, Texas: U.S. Air Force Center for Environmental Excellence.

Integrated Science & Technology Inc. 1997a. Summary of field activities. Hydrocarbon Vapor Migration Project. BP Oil Test Site, Paulsboro, New Jersey. Report to BP Oil, February 1997.

Integrated Science & Technology Inc. 1997b. Supplemental field activities. Hydrocarbon Vapor Migration Project. BP Oil Test Site, Paulsboro, New Jersey. Report to BP Oil, November 1997.

Johnson, P.C., and R.A. Ettinger. 1991. Heuristic model for predicting the intrusion rate of contaminant vapors into buildings. *Environmental Science & Technology* 25, 1445–1452.

Johnson, P.C., M.W. Kemblowski, and R.L. Johnson. 1999. Assessing the significance of subsurface contaminant vapor migration to enclosed spaces: Site specific alternatives to generic estimates. *Journal of Contaminant Hydrology* 8, 389–421.

Little, J.C., J.M. Daisey, and W.W. Nazaroff. 1992. Transport of subsurface contaminants into buildings. *Environmental Science & Technology* 26, 2058–2066.

Jeng, C.-Y., V.J. Kremesec, and H.S. Primack. 1996. Models of hydrocarbon vapor diffusion through soil and transport into buildings. In *Proceedings of the Petroleum Hydrocarbons and Organic Chemicals in Ground Water Conference*, 319–337. Westerville, Ohio: National Ground Water Association.

Jury, W.A., D. Russo, G. Streile, and H. El Abd. 1990. Evaluation of volatilization by organic chemicals residing below the soil surface. *Water Resources Research* 26, 13–30.

McAllister, P.M., C.Y. Chiang, J.P. Salinitro, I.J. Dortch, and P. Williams. 1995. Enhanced aerobic bioremediation of residual hydrocarbon sources. In *Intrinsic Bioremediation*, ed. R.E. Hinchee and J.T. Wilson, 67–75. Columbus, Ohio: Battelle Press.

Millington, R.J., and J.M. Quirk. 1961. Permeability of porous solids. *Transactions of the Faraday Society* 57, 1200–1207.

Nilsen, R.H., E.W. Peterson, K.H. Lie, N.R. Burkhard, and J.R. Hears. 1991. Atmospheric pumping: A mechanisms causing vertical transport of contaminated gases through fractured permeable media. *Journal of Geophysical Research* 96, 21933–21948.

Rifai, H.S., P.B. Bedient, R.C. Borden, and J.F. Haasbeck. 1987. *BIOPLUME II: Computer Model for Two Dimensional Transport Under the Influence of Oxygen-Limited Biodegradation in Groundwater, User's Manual.* Rice University, Houston, Texas: National Center for Groundwater Research.

Rifai, H.S., P.B. Bedient, J.T. Wilson, K.M. Miller, and J.M. Armstrong. 1988. Biodegradation modeling at aviation fuel spill sites. *Journal of Environmental Engineering* 114, 1007–1029.

Robinson, A.L., and R.G. Sextro. 1997. Radon entry into buildings driven by atmospheric pressure fluctuations. *Environmental Science & Technology*, 1742–1746.

Sanders, P.F., and A.H. Stern. 1994. Calculation of soil cleanup criteria for carcinogenic volatile organic compounds as controlled by the soil-to-indoor air exposure pathway. *Environmental Toxicology and Chemistry* 8, 1367–1373.

Schery, S.D., D.H. Gaeddert, and M.H. Wilkening. 1984. Factors affecting exhalation of radon from a gravelly sandy loam. *Journal of Geophysical Research* 89, 7299–7309.

Tsang, Y.W., and T.N. Narasimhan. 1992. Effect of periodic atmospheric pressure variation on radon entry into buildings. *Journal of Geophysical Research* 97, 9161–9170.

Unlu, K, M.W. Kemblowski, J.C. Parker, D. Stevens, P.K. Chong, and I. Kamil. 1992. A screening model for effects of land-disposed wastes on groundwater quality. *Journal of Containment Hydrology* 11, 27-49.

Unlu, K., J.C. Parker, and P.K. Chong. 1995. A comparison of three uncertainty analysis methods to assess groundwater impacts from land-disposed waste. *Hydrogeology Journal*, 3.

Zhang, W., E.J. Bouwer, A.B. Cunningham, and G.A. Lewandowski. 1995, Influence of sorption on organic contaminant biodegradation. In *Microbial Processes for Bioremediation*, ed. R.E. Hinchee, C.M. Vogel, and F.J. Brockman, 315–322. Columbus, Ohio: Battelle Memorial Institute.

## Biographical Sketches

***Jack Parker*** *is a distinguished research scientist at Oak Ridge National Laboratory in Oak Ridge, Tennessee. Previously, he served as president of Environmental Systems & Technologies Inc. for 12 years and as a professor of contaminant hydrology at Virginia Tech for 15 years. He has directed many research and consulting projects involving the modeling of subsurface contaminant transport in aqueous, gaseous and/or NAPL phases. His research has focused on the development and testing of models for multiphase flow and transport, remedial assessment and design optimization, risk assessment, inverse modeling, and analysis of model reliability. He has authored more than 200 technical publications and served on numerous expert panels, advisory and review boards, and delegations for government agencies, professional groups, private industry, and others. He has taught academic and short courses and presented workshops and invited seminars on modeling of subsurface organic contaminant transport in some 15 countries.*